Jun 1st, 12:00 AM

Experimental Study on Seismic Behavior of Industrial Storage Racks

Helmut Krawinkler

EXPERIMENTAL STUDY ON SEISMIC BEHAVIOR OF INDUSTRIAL STORAGE RACKS

By

Helmut Krawinkler*

INTRODUCTION

At any given time a large percentage of the movable goods in the United States is stored on industrial storage racks which usually consist of prefabricated cold formed steel elements assembled on site into various frame-type configurations. In the event of earthquakes these racks will be subjected to ground motions similar to those expected in building structures. Although it is debatable whether generally accepted seismic design criteria for building structures should be directly applied to storage racks, there is an evident need for a rational seismic design approach based on the same parameters that govern the response of building structures.

At this time very little is known about the structural response parameters governing the seismic behavior of industrial storage racks, such as lateral resistance and stiffness, as well as energy dissipation through damping and inelastic deformations. A thorough study of these parameters is needed to evaluate the dynamic response of storage racks from which a simplified design methodology can be developed. It appears most rational that this simplified design method be based on equivalent static lateral forces derived from a base shear equation of the UBC type

---

*Assistant Professor of Civil Engineering, Stanford University

$$V = ZKCW \quad (1)$$

where K and C need not necessarily be identical to presently used values for building structures. In particular, the value of K should be based on a rational evaluation of ductility and energy dissipation capacity of rack configurations.

Discussed in this paper is an experimental study on the seismic behavior of industrial storage racks which has the following specific objectives:

1. Investigation of the strength and stiffness characteristics of frame-type racks and their components under lateral loads.
2. Development of mathematical models for the load-deformational response of rack components.
3. Determination of the dynamic characteristics of racks (frequencies, mode shapes, and damping).
4. Study of energy dissipation characteristics which should aid in the determination of the factor K in Equation 1.

One specific rack configuration was selected for this study, namely, the standard pallet rack. These racks consist of semi-rigid moment resisting frames in the longitudinal direction and braced frames in the transverse direction. Two types of racks were studied, both of similar geometric configuration (two bays long, one bay deep, and three levels high, see Fig. 1), but built with different structural shapes and beam-to-post connections.

The purpose of this paper is primarily to identify the response parameters of importance in the seismic response of these racks, to discuss the types of experiments and the experimental procedures recommended for

the evaluation of these response parameters, to discuss mathematical modeling based on experimental results, and to present conclusions that can be drawn from experimental results on the behavior of industrial storage racks under various levels of seismic excitations.

RESPONSE PARAMETERS

To achieve a correlation between analytical response prediction and the true dynamic response of structures, experimental research needs to be directed towards defining each term in the discretized equation of motion

$$[M]\{\ddot{u}\} + [C]\{\dot{u}\} + [K]\{u\} = [M]\{\ddot{u}_g\} \qquad (2)$$

where, assuming that the motion $\{\ddot{u}_g\}$ at the base of the structure is known, [M] ideally should represent the proper mass distribution throughout the structure; [C] ideally should represent all damping contributions which cannot be included with confidence in the formulation of the [K] matrix; and [K] ideally should represent all stiffness characteristics of the structure, including geometry and material nonlinearities, stiffness degradations, and time dependent effects.

To apply these considerations to industrial storage racks, several characteristics of such cold-formed steel structures need to be pointed out.

The pallet beams which usually consist of stiff sections with high moment capacity are connected to perforations of the upright posts by means of grip-type mechanical connectors. The beam-to-post connections do not behave as rigid connections since distortions can occur in the walls of the posts at the joints and in the connectors themselves.

Consequently, relative rotation takes place between posts and beams which can be modeled closely by rotational springs at the joints. In most practical cases these springs are nonlinear and rather flexible and have an ultimate moment capacity which is less than the flexural capacity of the beam sections. Hence, strength and stiffness of pallet beams under lateral loads are usually controlled by the response characteristics of the beam-to-post connections.

Thus, the strength parameters which need to be studied experimentally are the ultimate moment capacities at the beam-to-post connections for positive and negative bending as well as moments for an "allowable stress" or "service load" level. The latter moments are needed for a rational allowable stress or service load analysis and design which needs to be based on elastic behavior of the structure.

The upright posts usually consist of C-shaped thin-walled sections subjected to axial loads and bending moments. Under axial loads these posts may fail in either flexural or torsional-flexural buckling, while the interaction between axial loads and bending moments can be treated by means of M-P interaction diagrams.

Stability considerations will play a significant part in the seismic response of industrial storage racks. In the transverse direction the posts and the bracing members will be subjected to high axial forces and buckling can occur in the bracing members due to excessive horizontal story shears and in the posts due to overturning effects. However, these high shears and overturning moments will develop only in lagged racks (bolted to the floor) where the base plates can transmit the necessary uplift forces to the posts. In the longitudinal direction overturning moments will be relatively small and possible buckling in

the posts will depend primarily on the amount of vertical load on the racks. However, in this direction the semi-rigid frames may be subjected to large lateral drifts and P-δ effects may greatly amplify the moments attracted by beams and posts and may also lead to dynamic instability problems.

Member stiffnesses are needed for the computation of internal force distribution as well as period and drift calculations. The elastic stiffnesses of pallet beams, posts, and transverse bracing systems can confidently be predicted analytically, but the stiffness of the beam-to-post connections can only be obtained from experiments. Also, the degree of fixity that can be achieved by bolting the post base plates to the floor needs to be studied experimentally.

Horizontal diaphragm action will affect the dynamic response and force distribution in the racks. Only few racks have horizontal bracing systems, but partial diaphragm action will be developed through pallets and pay load.

Like most other structures, industrial storage racks must rely on energy dissipation through inelastic deformations in the event of severe earthquakes. Measures of this energy dissipation capacity are member ductility as well as size, shape and stability of the hysteresis loops obtained under cyclic loading.

The level of forces attracted in structures during seismic excitations will also depend on the damping in the structure and the pay load. Although the damping from the pay load can be significant, this parameter was not included in the scope of the reported study. The structural damping which will come primarily from the beam-to-post connections will be strongly amplitude dependent and will be affected by the looseness of the connections.

The parameters discussed in this section were investigated in the experimental study reported in this paper. Monotonic as well as quasi-static cyclic loading tests were carried out on structural elements, subassemblies and full-size rack assemblies. All tests were carried to failure or, where failure did not take place, to deformation levels which are larger than those expected in severe earthquakes. The configurations selected for element and subassembly tests were the same as those used by Pekoz in previous studies at Cornell University (1.2). Four full-size racks were tested to study the interactions taking place between the individual elements under loading conditions similar to those expected in severe earthquakes. Essentially, the test configurations closely follow those outlined in Ref. 3.

In addition to these quasi-static tests, two of the full-size racks were also subjected to forced vibrations induced by means of an electromagnetic vibration generator. These tests resulted in information on damping properties, natural frequencies and mode shapes for longitudinal, transverse and torsional vibrations.

EXPERIMENTAL SET-UP AND TEST PROCEDURES

Selection of Test Specimens. The choice of feasible test specimens will largely determine the outcome of any experimental study. Boundary conditions and load application for components and subassemblies must be selected properly to simulate actual internal force distribution and interactions between the individual components. In the response of industrial storage racks the critical elements were found to be the beam-to-post connections and the posts themselves. The cantilever and portal tests described in the next section are needed for a study of beam-to-post connections. The simple cantiliver tests give reliable results

for moment-rotation behavior at the joints for only one specific value of moment to shear ratio in the beams. The actual moment to shear ratio in pallet beams under combined vertical and lateral loads will be different from that used in the cantilevers. Since it is expected that this ratio will have an effect on the moment-rotation relationship at the joints, it was decided to test simple portal frames which will properly simulate the field conditions.

The behavior of posts for lateral loads in the longitudinal direction will strongly depend on the joint restraints provided by the pallet beams which will determine the effective column length. It was impossible to design a subassembly test which permitted proper simulation of boundary and loading conditions for posts. This together with the need for an investigation of P-δ effects made it necessary to test full size frame assemblies with lateral loads applied in the longitudinal direction. Tests on full size rack assemblies with lateral loads in the transverse direction were also needed to study the response of the braced transverse frames (see Fig. 1).

Load Application and Loading Histories. In all subassemblies and full-size racks the pay-loads were simulated by 1000 lb. concrete blocks placed on standard wood pallets. Lateral loads were applied by means of a hydraulic actuator attached to the structures in a manner which closely simulates the effects of inertia forces from horizontally accelerated pay-loads. The loads were applied quasi-statically to permit accurate force and displacement control and the recording of visual observations. Since the natural frequencies of storage racks are low, the strain rate effects due to dynamic excitations are small and quasi-static load application will not significantly distort strength and ductility characteristics.

Rather subjective decisions had to be made regarding the choice of representative loading histories for cyclic loading tests. Basically, two types of loading histories had to be considered, one leading to low cycle fatigue failure (symmetric displacement cycles) and one leading to incremental collapse (displacements predominantly in one direction). Because of the importance of the P-δ effect in longitudinal excitations of storage racks, it is anticipated that lateral displacements will increase in the direction of the first large acceleration pulse leading to incremental collapse type problems. Nevertheless, it was decided to apply loading histories with symmetric cycles of step-wise increasing displacement amplitudes. Three cycles of equal displacement amplitude were carried out in each step. It is believed that such loading histories are critical for steel structures, since cyclic stress reversal will accentuate local instability problems and initiation as well as propagation of cracks in weldments and base materials.

Instrumentation, Recording, and Data Reduction. Since the load-deformational response at the beam-to-post connections is nonlinear and affected by the looseness of the connections, it was decided to obtain continuous analog records of all important response parameters by means of X-Y recorders and strip-chart recorders. The analog records were then digitized electronically on a digitization table for data manipulation on a mini-computer. The final results of the experimentally obtained and analytically derived response parameters were stored on magnetic tape and graphically displayed on a Cal-Comp Plotter.

In the dynamic tests the analog acceleration signals were digitized instantaneously in an A to D converter and data analysis was carried

out by means of an on-line Fourier Analyzer system.

The instrumentation system consisted of electronic sensors for the measurement of loads (load transducers), displacements (LVDT's and Linear Potentiometers), rotations (RVDT's), accelerations (accelerometers), and strains (resistance strain gauges). The evaluation of the experimental data showed that all pre-calibrated sensors gave consistent and reliable results. However, strain gauge arrangements which were not calibrated against known moments and axial forces could only be used for qualitative evaluations. Due to the small thickness of the structural elements and the presence of perforations in the posts it was not possible to establish a reliable relationship between strains and internal forces based on simple elastic beam theory.

ELEMENT TESTS

The distortions at the beam-to-post connections will lead to relative rotations between beams and posts which can be represented by rotational springs. The moment-rotation (M-θ) relationship for these springs was determined from cantilever tests of the type shown in Fig. 2 (see also Ref. 2).

Two methods were employed to determine the spring rotation at the center of the joint. Experimentally, θ was obtained as the difference between rotation measurements taken at the center of the joint and the centerline of the beam adjacent to the connectors. Alternatively, θ can be obtained from the measured value of the tip deflection δ and computations of the elastic beam deflections δ_b and the column rotation θ_c, i.e.

$$\theta = \frac{\delta - \delta_b}{\ell_b + \frac{d_c}{2}} - \theta_c \tag{3}$$

where

$$\delta_b = \frac{P(\ell_b + \frac{d_c}{2})^3}{3EI_b} \tag{3a}$$

$$\theta_c = \frac{P(\ell_b + \frac{d_c}{2})\ell_c}{16EI_c} \tag{3b}$$

The dimensions used in these equations are shown in Fig. 2, I_b and I_c are moments of inertia of beam and column, respectively, and P is the applied load.

The rotations obtained from these equations are not exact since centerline dimensions are used. However, since it is expected that centerline dimensions will be used in analytical studies, it is consistent that the mathematical model for the artifical rotational spring at the joint also be based on centerline dimensions.

Figure 3 shows the M-θ relationships of two types of specimens for positive and negative bending as obtained from Eqs. (3). It can be seen that strength and stiffness vary significantly for positive and negative bending and from specimen to specimen. The looseness of the connections often led to very small initial stiffnesses which suggests the application of a small pre-load in experiments where continuous records cannot be obtained. In some cases it will be difficult to define a suitable linear range for elastic analysis and design. Hence, service load design will have to be based on allowable moments (as a percentage of the ultimate moment capacity)

and an average stiffness which should not vary substantially within the allowable range of moments.

Reasonable good agreement (within about 10%) was obtained between the experimentally measured rotations and those computed from Eqs. (3). This shows that the analytical model for computing rotations is adequate and rotation measurements may not be necessary in future experimental studies.

SUBASSEMBLY TESTS

To study the interaction between pallet beams and upright frames in realistic situations, the single-bay portals shown in Fig. 4 (see also Ref. 2) were tested under simultaneous vertical and lateral load application. Vertical loads representing service live loads were simulated with concrete blocks resting on standard wood pallets. The lateral load was applied at the center of a distribution plate which distributed the load equally to the two pallet beams.

As expected, the response of the portals to lateral loads was governed by strength and stiffness of the beam-to-post connections. The moment-rotation relationships of the individual joint springs can be extracted from experimental data provided that the shear forces in the individual posts can be determined. Since strength and stiffness of the connections may differ significantly for positive and negative bending, the two posts in general will not attract equal shears. To evaluate the shear forces in the posts, two sets of strain gauges were placed on the pallet beams close to the connections. Identical sets of strain gauges were used in the cantilever tests which permitted a calibration of strain vs. moment. From the known moments at the

strain gauge locations the moments at the centers of the beam-to-post joints and the shears in the posts can be calculated.

The relative rotation θ between beam and post was measured with rotation gauges and also calculated based on elastic behavior of beams and posts. Very good correlation was obtained between measured and calculated values. Based on elastic behavior of beams and posts, the rotation θ can be computed from

$$\theta = \frac{\delta - \delta_c}{h} - \theta_b \tag{4}$$

where

$$\delta_c = \frac{Mh^2}{3EI_c} \tag{4a}$$

$$\theta_b = \frac{\ell}{6EI_b(M + \overline{M})^2}(2M^3 - \overline{M}^3 + 2M^2\overline{M}) \tag{4b}$$

The dimensions used in these equations are shown in Fig. 4, δ is the lateral deflection at the beam centerline, M is the moment due to lateral load plus the P-δ effect at the joint where rotations are computed, and $\overline{M}$ is the moment at the opposite joint.

Figure 5 shows in solid lines the M-θ relationships for the two joints of a Type B specimen as obtained from Eqs. (4). The origin of this graph corresponds to the moments caused by vertical loads. The discrete points marked on the diagrams show the difference in moments and rotations at the two joints for specific values of lateral loads. When the M-θ diagrams are compared with those obtained from cantilever tests (Fig. 3), it can be seen that the diagrams are similar in shape and moment capacity, however, the diagrams from the portal tests exhibit

a significantly higher initial stiffness. This proves that the stiffness depends on the shear to moment ratio in the beams which is significantly higher in the portals due to the presence of vertical loads. Thus, it should be noted that the portal tests are more appropriate than cantilever tests for an experimental determination of the joint spring characteristics.

However, the accuracy of the M-θ relationships for individual joints obtained from portal tests depends strongly on a precise measurement of beam moments which is difficult to achieve. For industrial testing, the simple cantilever test which requires only load and displacement measurements should give sufficiently accurate results for strength and stiffness of individual joints. The portal test could be utilized to obtain average values for moment-rotation characteristics considering both joints in the portal. These average values characterize the overall lateral resistance and stiffness of pallet beams in frame configurations, which are parameters that should prove useful for the development of seismic design criteria. The average moment at the two joints can be expressed as

$$\overline{M} = \frac{H}{2}h + P\delta \tag{5}$$

and the average rotation, assuming that the moments due to a lateral load are equal at the two joints, is given by

$$\overline{\theta} = \frac{\delta}{h} - \frac{\overline{M}h}{3EI_c} - \frac{\overline{M}\ell}{6EI_b} \tag{6}$$

where H is the lateral load applied to one portal frame, and P is the axial force in the post due to vertical loads.

The $\overline{M}$-$\overline{\theta}$ relationship obtained from Eqs. (5) and (6) is shown dashed in Fig. 5.

In Fig. 6 are presented the lateral load-deflection diagrams (H-δ) of two

Type A portal frames, one tested with half live load, the other with full live load. Despite the large difference in pay-load, the response to lateral loads is rather similar. This is characteristic for frames with flexible connections where the end moments due to vertical loads are small compared to moments caused by lateral loads.

Figure 7 shows the H-δ diagram of a Type B portal frame which was subjected to cyclic loading histories. It is interesting to note that the hysteresis loops are similar in shape to those obtained in reinforced concrete flexural members with high shear. The looseness of the connections and localized yielding at the connections caused by previous loading led to a pinching of the hysteresis loops similar to that caused by shear transfer in reinforced concrete. It was observed that for constant displacement amplitudes the second load cycle led to a decrease in the area enclosed by the hysteresis loop while the third load cycle was practically identical to the second one.

At the displacement amplitude where failure initiated (in this case cracking at the welds between the beams and the connectors at a displacement amplitude of 1.5 in. [3.81 cm]), subsequent load cycling led to a pronounced decrease in strength and hysteresis area. It should be emphasized that the cracking at the welds in the cyclically loaded specimen occurred at smaller displacements than in the monotonically loaded specimen. This indicates that the strength and ductility obtained from monotonic loading tests may not be fully representative for the load-deformational response characteristics under seismic excitations. For illustration, the H-δ diagram for an identical, monotonically loaded Type B portal frame (Specimen B-P-1) is also shown in Fig. 7.

FULL-SIZE RACK TESTS

Three-story rack assemblies were tested to study the interaction between pallet beams, posts and connections under gravity loads and seismic effects simulated by quasi-static cyclic load application at the level of the pallet beams on the third story.

Longitudinal Load Tests. Two assemblies were tested with the lateral load applied in the longitudinal direction as shown in Fig. 8. In this direction the rack assemblies act as moment resisting frames with semi-rigid connections. One rack assembly (Type A) was loaded with half of the rated pay-load (3000 lbs. [13.35 kN] per bay at each level), the other (Type B) with full pay-load. The racks were subjected to cyclic loading with displacement amplitudes of 1, 2, 4 and 6 in. (2.54, 5.08, 10.16 and 15.24 cm), respectively. Three symmetric cycles were carried out at each displacement amplitude. The loading arrangement did not permit cyclic loading beyond a displacement of 6 in. (15.24 cm), but loading was continued monotonically until either failure occurred or the displacement limit of the loading arrangement was reached.

The lateral load-displacement history for one frame of the Type A rack is shown in Fig. 9. The dimensions of this rack are given in Fig. 1. The M-θ relationships for the joint springs are shown in Fig. 3, and the moment of inertia for the pallet beams is 2.664 in.^{4} (110.9 cm^4). The C-shaped column sections have the following section properties: moment of inertia about axis of bending, I_x = 1.037 in.^{4} (43.16 cm^4), elastic section modulus, S_x = 0.691 in.^{3} (11.32 cm^3), plastic section modulus, Z_x = 0.84 in.^{3} (13.77 cm^3), cross-sectional area, A = 0.67 in.^{2} (4.32 cm^2), and radii of gyration, R_x = 1.228 in. (3.12 cm) and R_y = 0.688 in. (1.75 cm). The yield strength specified

by the manufacturer is F_y = 50 Ksi (34.5 kN/cm^2).

The following observations of general interest for the seismic behavior of industrial storage racks were made in this experiment:

1. Because of the nonlinear behavior of the beam-to-post connections, the load-deformational response of the rack had only a very small linear range.

2. The hysteresis loops are stable but show the characteristic pinching (decrease in stiffness close to zero load) as was discussed already in the section on subassembly tests.

3. The relative strengths of beams and posts are such that post behavior will determine the maximum resistance to lateral loads. Failure was expected due to combined action of axial load and bending moment at the center post. However, in this case the axial load was too small (4700 lbs. = 20.9 kN) to affect significantly the capacity of the post. Consequently, flexural plastic hinges developed in the center post above and below the beam-to-post connection, leading to a very ductile response of the rack assembly. At the maximum recorded deflection of 17.3 in. (43.9 cm) no sign of failure could be detected. After formation of the plastic hinges at the center posts, moment redistribution to the exterior posts accounted for the additional increase in lateral resistance. The large rotations at the plastic hinges in the center post can be seen in the photo shown in Fig. 10.

4. Because of the low lateral stiffness of the semi-rigid frames, the P-δ effect is significant and should not be neglected in response predicitons. When the P-δ effect is replaced approximately by an equivalent story shear, $\overline{V} = P\delta/h$ (δ = story displacement, h = story height), it can be shown that in the tested Type A rack assembly the P-δ effect

amplified the story shear in the first story by a factor which is equal to 1.17 for the initial linear range and becomes as high as 1.86 at the maximum displacement of 17.3 in. (43.9 cm).

5. At all levels of lateral loads a significant rotational restraint was provided by the base plate to floor connections. Strain gauge readings in the center post showed that at all levels of lateral loads the moment in the post at the base plate was at least equal to 60 percent of the moment at the beam-to-post joint. Since the development of this moment at the base will greatly reduce the moment in the post below the first floor joint (in this example by about 35 percent), it will be quite beneficial to include the base restraint in mathematical models.

6. The equivalent shear ($H + P\delta/h$) in the first story at the maximum recorded displacement was 65 percent higher than the ultimate shear capacity predicted analytically. The main reasons for this large difference are: (1) the prediction of the strength capacity of the posts was based on a conservative M-P interaction diagram obtained by drawing a straight line between the plastic moment capacity on the M-axis and the buckling load on the P-axis; (2) when the strength capacity of the center post was attained, failure did not occur which permitted a redistribution of moments to the exterior posts; (3) the rotational restraint at the base plate to floor connection was not included in the analytical model; and (4) strain hardening did cause an increase in the moment capacity at plastic hinges.

In the cyclic load test of the Type B rack, which was loaded with full pay-load (6000 lbs. [26.7 kN] per bay at each level), buckling at the center post was imminent at a lateral displacement of 9.0 in. (22.9 cm). However, this buckling occurred at approximately 3 times

the displacement and 1.85 times the equivalent shear capacity predicted analytically. This again indicates that the combined moment-axial load capacity is higher than that predicted from a straight-line M-P interaction diagram and that also in this case moment redistribution did take place.

Transverse Load Tests. Two rack assemblies of the type shown in Fig. 11 were tested with lateral loads applied in the transverse direction. In this direction the lateral load resisting units are braced frames as shown in Fig. 1. The horizontal load was distributed equally to the two upright frames by means of a distribution beam. Since it was intended to test the behavior of interior bays with zero moments in the posts in the longitudinal direction, 1000 lb. concrete blocks were suspended from cantilever beams (see Fig. 11) to equilibrate the beam moments at the joints. In this manner the loading condition of interior bays with half pay-load was simulated. Knee braces were added to prevent displacements in the flexible longitudinal direction.

Figure 12 shows the horizontal load-deflection response for one transverse frame of the Type A rack assembly. In this case force control was employed for the cyclic load application since the response was expected to be close to linear. Three load cycles each were carried out with load increments of 1000 lbs. (4.45 kN).

As can be seen from Fig. 1, the diagonal braces were connected eccentrically to the posts causing significant weak axis bending in the posts. This bending in combination with high axial loads accounted for some of the inelastic behavior exhibited in Fig. 12. However, most of the inelastic action came from local bending of the 1/4 in. (0.64 cm) thick base plates at the post-to-floor connections. Because of the large

height to width ratio of the upright frames (equal to 4.4), uplift forces developed in one of the posts when the lateral load on the frame exceeded approximately 1000 lbs. (4.45 kN). These uplift forces had to be transferred from the post to the anchor bolt through flexural action of the base plate. This flexural action limited the lateral force transfer in this rack assembly, since rather brittle fracture occurred at the weld connecting the post to the base plate before the buckling loads in posts or braces were attained. Here again it should be noted that the lateral load causing failure at the weld was approximately 45 percent larger than the analytically predicted maximum lateral load based on the strength capacity of the posts.

DYNAMIC TESTS

Natural frequencies, mode shapes, and damping characteristics of the two-bay three-level racks were obtained from forced and free vibration tests. Forced vibrations were generated by means of an electromagnetic vibration generator placed on top of the structure. Sinusoidal excitations were used for damping measurements and band-width limited white noise was used for the investigation of frequencies and mode shapes.

Two accelerometers were used for response measurements. One accelerometer was mounted at a reference point while the other was placed at various predetermined locations for mode shape determination. Two time histories were recorded simultaneously and the Fourier transform as well as the auto- and crosspower spectral density functions were calculated. All computations were done on-line with a Fourier Analyzer System. To minimize random and recording errors, the while noise excitation was repeated fifty times for each recording station and average values

for auto- and crosspower spectra were obtained. The transfer function for the two time histories was then calculated as the ratio of the average crosspower spectral density function over the average autopower spectral density function at the reference point. The values of the transfer function at the spectral peaks determine the relative modal accelerations and displacements.

Figure 13 shows the average autopower spectral density functions at the reference point (exterior beam-to-post joint at the third level) for longitudinal and transverse excitations of the Type A rack. While the three longitudinal frequencies are easy to identify, a large number of spectral peaks are evident for transverse excitation. From the aforementioned mode shape calculations, peaks 1 and 3 were identified as basic transverse modes, while peaks 2, 4, and 6 represent torsional modes. Peak 5 was identified as a horizontal mode with the center frame moving opposite to the exterior frames. From the high frequency of this mode (7.3 Hertz) it can be concluded that significant diaphragm action was provided by the wooden pallets loaded with concrete blocks.

The free vibration studies showed that damping was strongly amplitude dependent. This was to be expected from the nonlinear characteristics of the beam-to-post connections. Fig. 14a shows the decay in first mode longitudinal vibration. The damping estimated from the changes in the logarithmic decrement between individual peaks is shown in Fig. 14b. The oscillations in the damping values were caused by a beats phenomenon. Although these damping values are only approximate, they indicate a rapid increase in damping at acceleration amplitudes above one percent.

CONCLUSIONS

The objective of the experimental study reported herein was to acquire basic information on the response characteristics that govern the seismic behavior of industrial storage racks. Although the study was limited to two types of standard pallet racks, it can be expected that much of what has been learned can be applied to other rack configurations. The purpose of the study was to acquire information which, together with results from shaking table tests carried out at the University of California, Berkeley, can serve as a basis for the development of seismic design criteria for storage racks.

The conclusions drawn from this study, which should only be applied to racks of similar configurations, are as follows:

1. The elements which control the seismic response of storage racks are the beam-to-post connections, the upright frames consisting of posts and bracing members, and the frame-to-floor connections.

2. The behavior of the beam-to-post connections can be represented by rotational springs whose characteristics should be determined experimentally. Ideally, strength, stiffness and ductility of these springs should be determined by means of subassembly (portal) tests using cyclic loading. The cantilever test, which is much simpler to carry out and results in more reliable measurements of moments, could be used as an alternative.

3. The determination of the response characteristics of posts and upright frames will require tests of rack assemblies which permit proper simulation of boundary and loading conditions.

4. Mathematical models presently used for predicting the strength of posts under combined actions of axial load and bending moments appear to be very conservative.

5. The P-δ effect greatly affects the lateral strength and stiffness in the longitudinal unbraced frame direction and should be included in response predictions.

6. Because of local deformations at the beam-to-post connections, hysteresis loops have a pinched shape similar to that obtained in reinforced concrete elements with high shear.

7. Low cycle fatigue phenomena (in particular, early fracture at welds or points of stress concentrations, caused by strain reversals) may affect the strength and ductility of beam-to-post and post-to-floor connections.

8. The ductility and energy dissipation capacity of racks is much larger in the longitudinal (moment resisting frame) direction than in the transverse (braced frame) direction.

9. The ductility of the longitudinal frames depends strongly on the ratio P/P_{cr} (P = axial load, P_{cr} = buckling load) in the individual posts. For small P/P_{cr} ratios, column buckling will not take place and ductile plastic hinges will develop in the posts.

ACKNOWLEDGEMENTS

This experimental study was part of a project on the development of seismic design criteria for industrial storage racks, sponsored jointly by the National Science Foundation and the Rack Manufacturer's Institute, with J. A. Blume as principal investigator and R. E. Scholl as project manager. The work was carried out in the John A. Blume Earthquake Engineering Center at Stanford University.

The participation of Dr. C. Kircher who completed the dynamic testing,

and the skillful assistance of the graduate students M. Astiz, N. Cofie, and B. Lashkari-Irvani is gratefully acknowledged.

APPENDIX -- NOTATION

d_c = depth of column (post)

E = modulus of elasticity

h = height of story

H = lateral load

I_b, I_c = moment of inertia of beam and column (post), respectively

ℓ = center-to-center span in longitudinal direction

ℓ_b, ℓ_c = length of beam and column, respectively, in cantilever test setup

M = moment at center of beam-to-post joint

P = sum of axial forces in posts (P-δ effect)

δ = total deflection

δ_b, δ_c = elastic deflection of beam and column, respectively

θ = spring rotation

θ_b, θ_c = elastic rotation of beam and column, respectively, at center of beam-to-post joint

REFERENCES

1. Pekoz, T., "Interpretation of Pallet Rack Test Results," Report to the Rack Manufacturers Institute; Ithaca, Feb. 1978.

2. Pekoz, T., "Pallet Rack Design Criteria," Report to the Rack Manufacturers Institute; Ithaca, Feb. 1978.

3. Rack Manufacturers Institute, "Specification for the Design, Testing, and Utilization of Industrial Steel Storage Racks," March 1977.

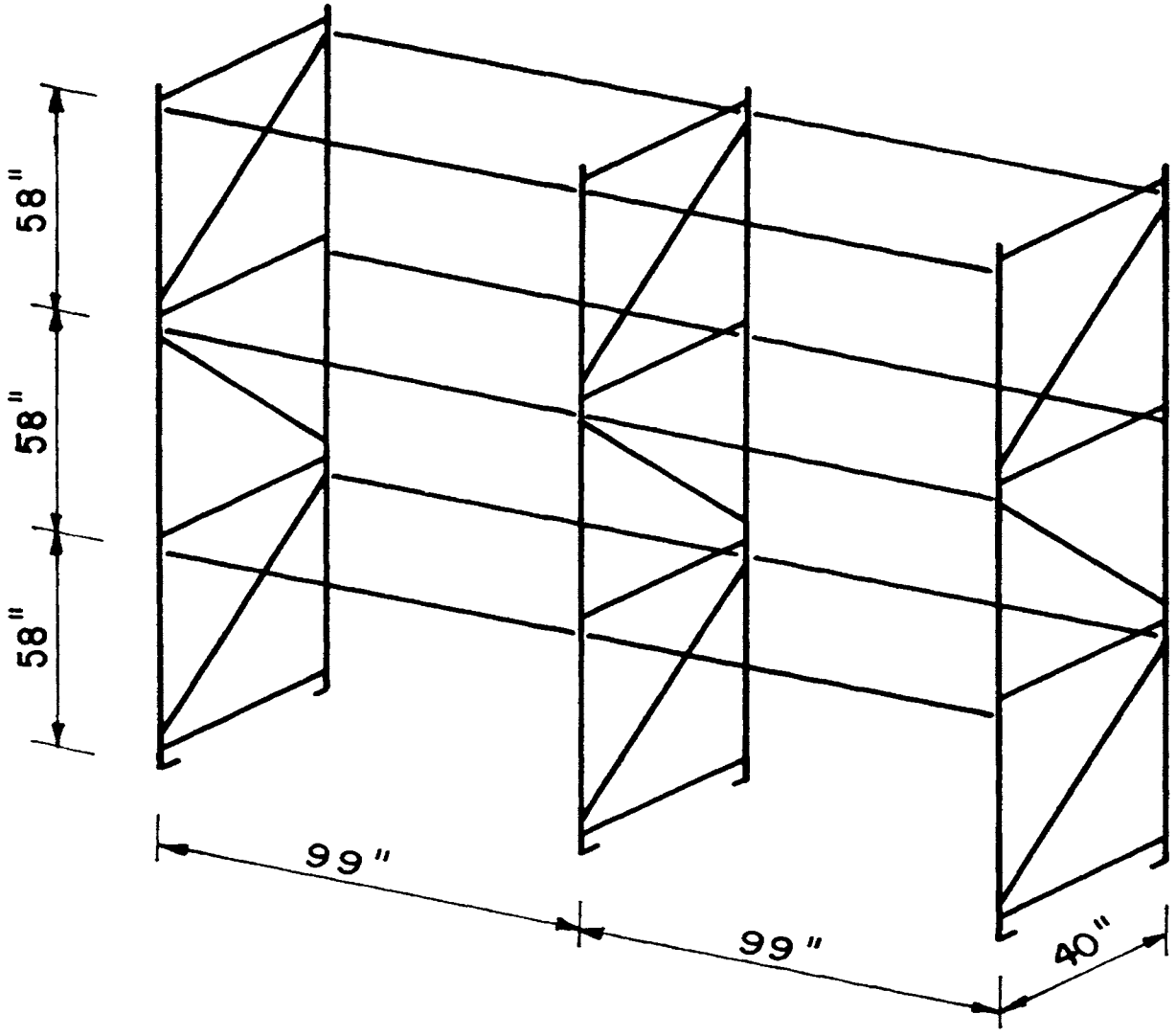

Fig. 1. Rack Configuration

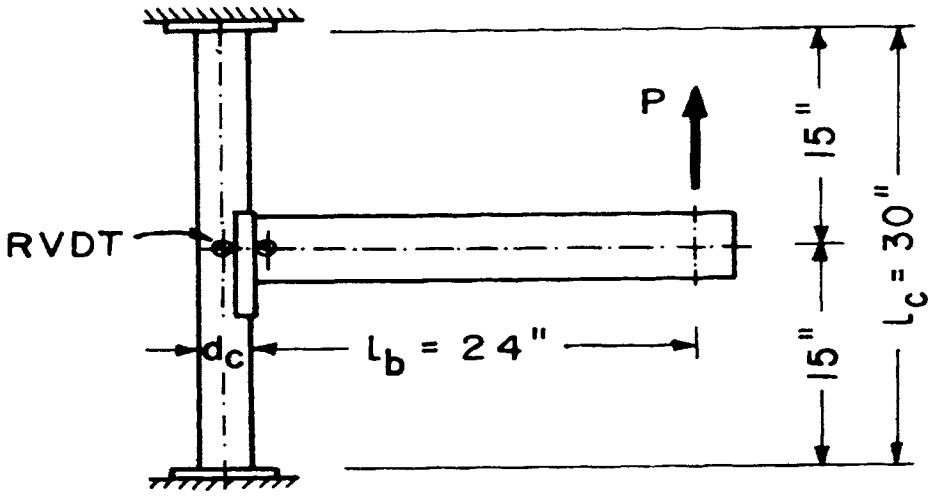

Fig. 2. Cantilever Test Setup

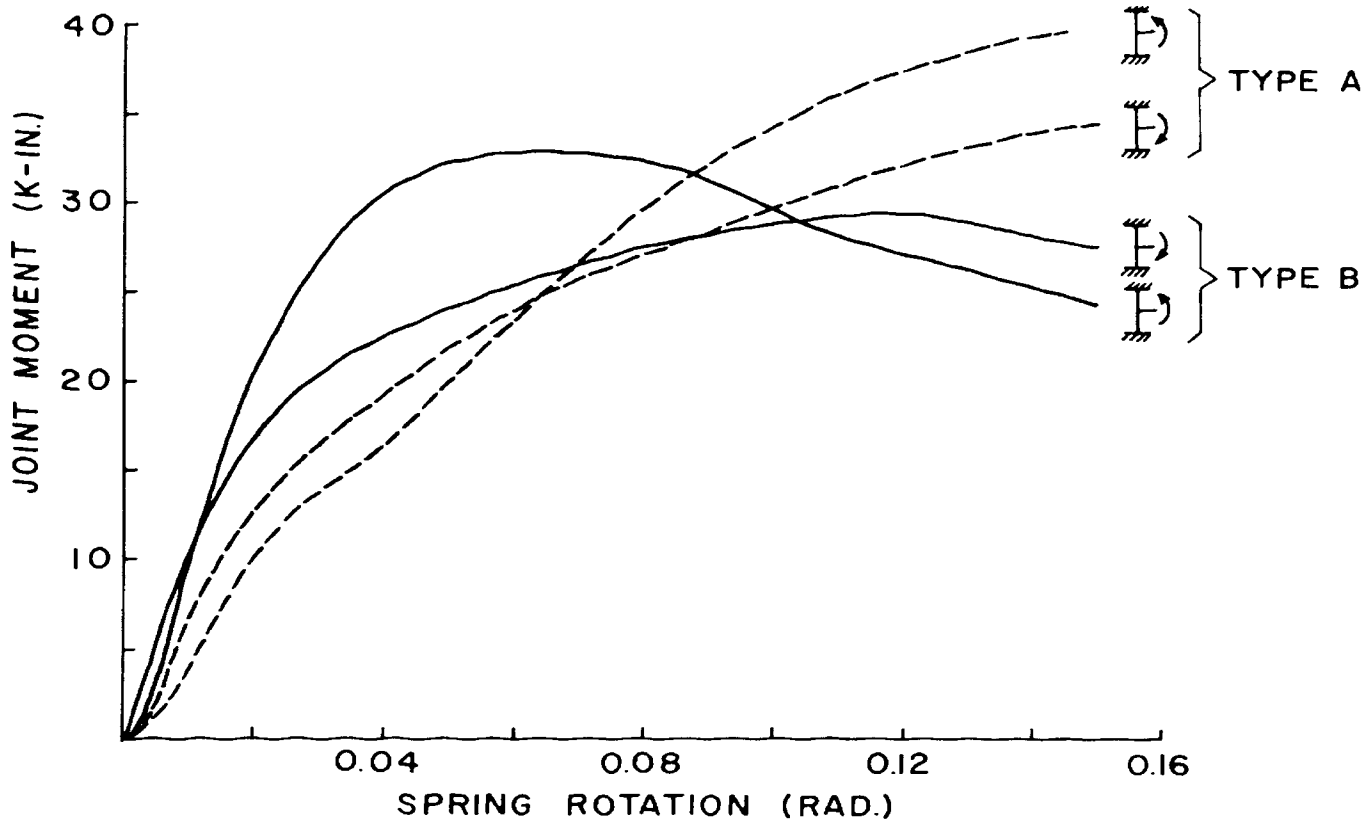

Fig. 3. M-θ Relationships -- Cantilever Tests

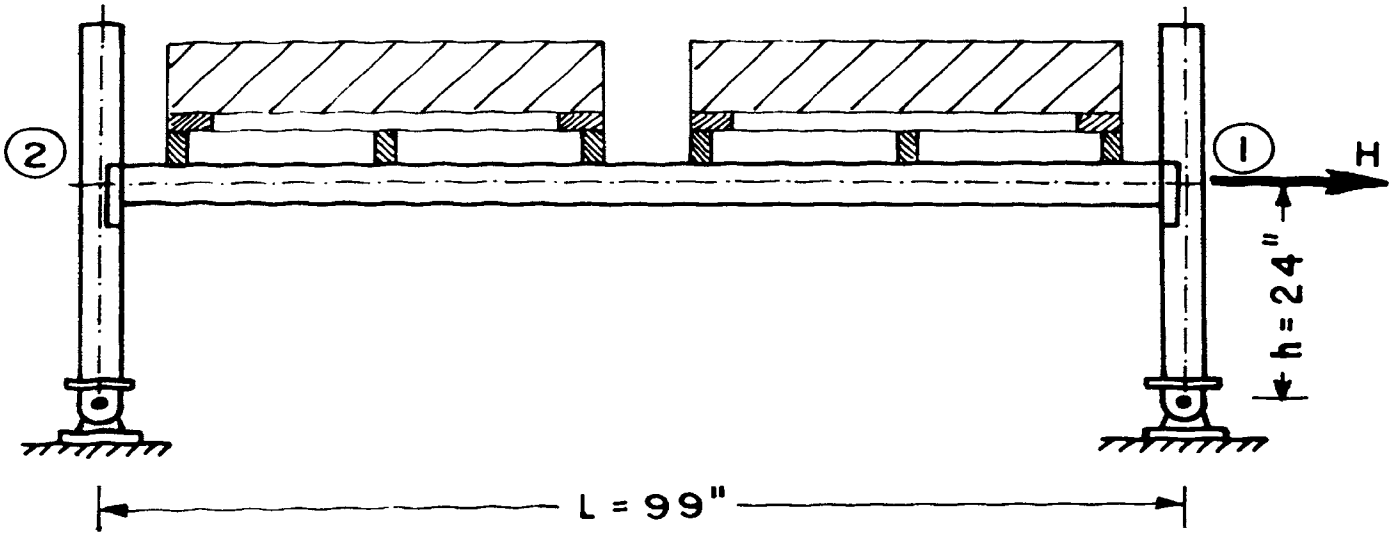

Fig. 4. Portal Frame -- Test Setup

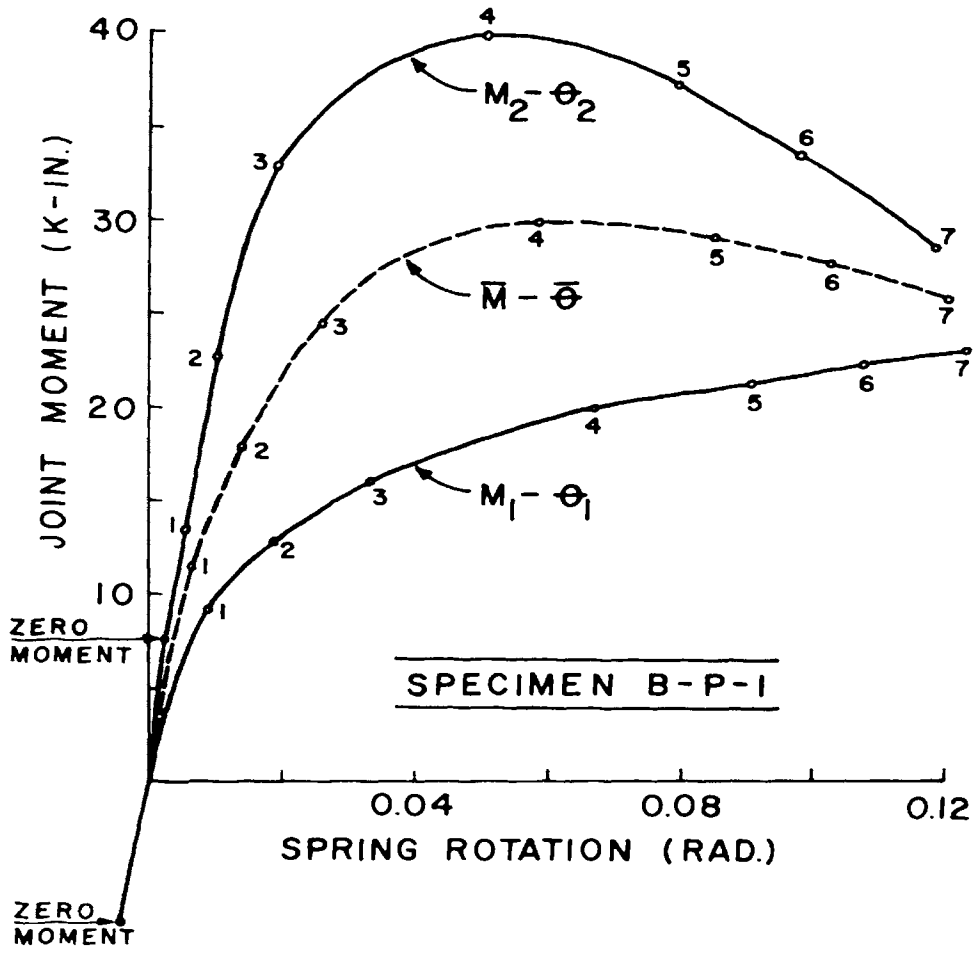

Fig. 5. M-θ Relationships -- Portal Tests

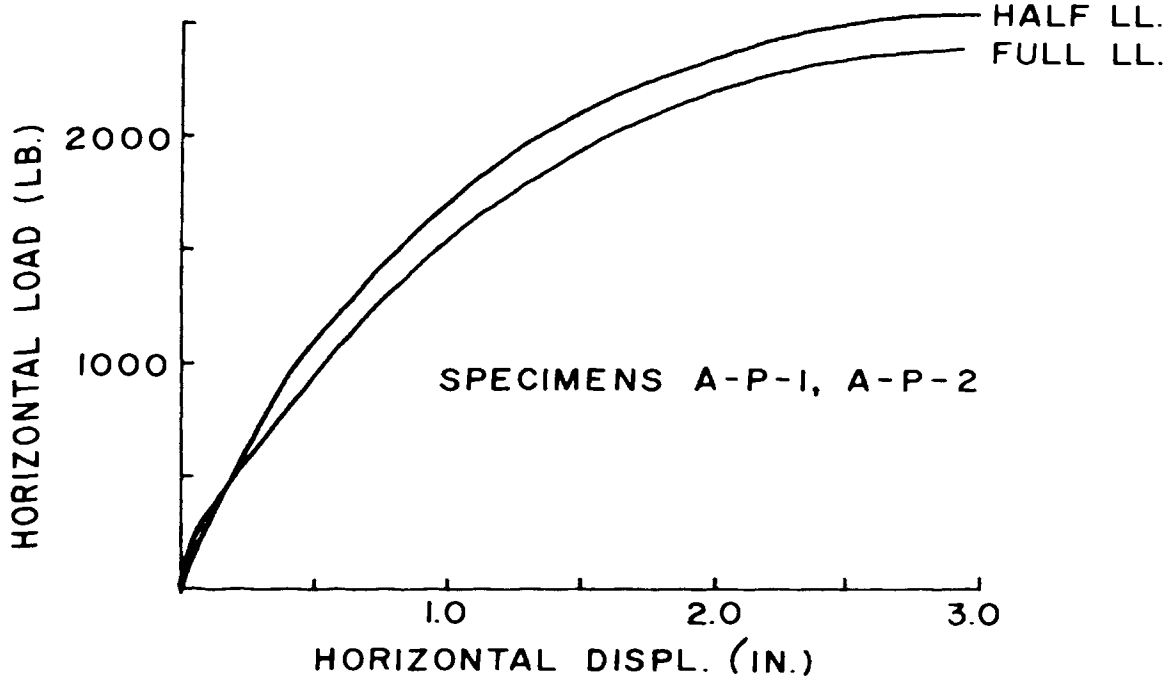

Fig. 6. H-δ Relationships -- Portal Tests

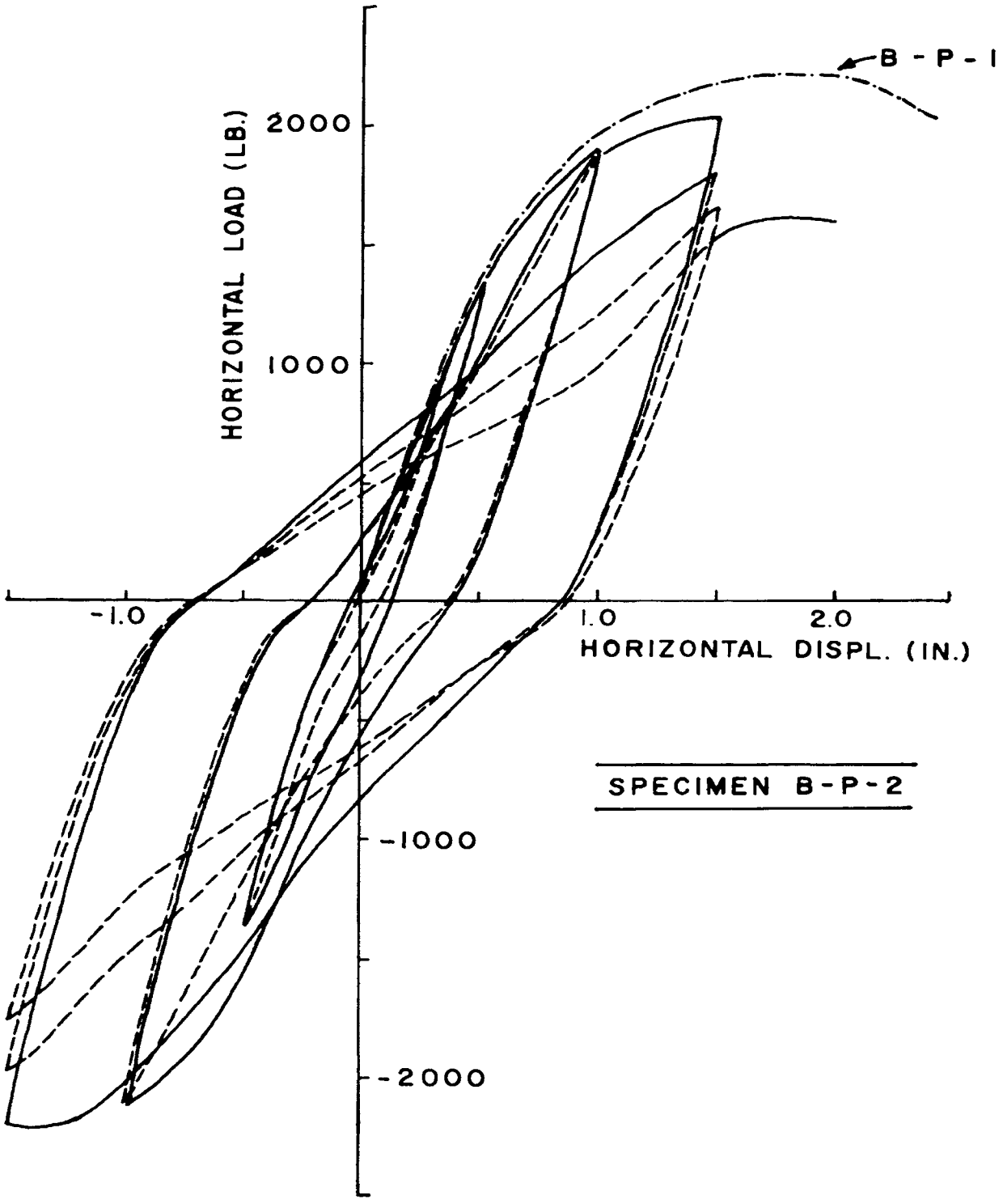

Fig. 7. H-δ Relationship for Cyclic Loading -- Portal Test

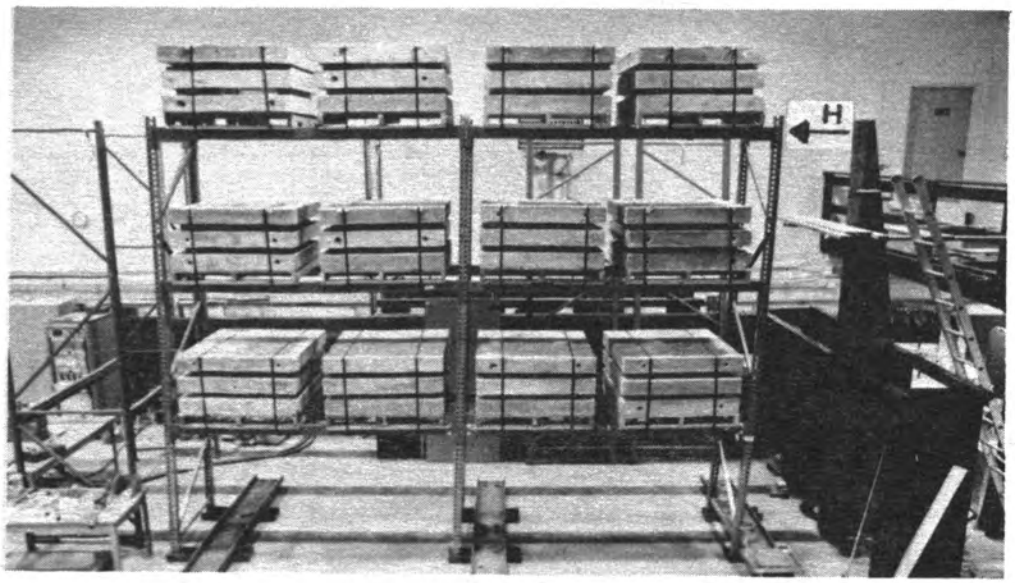

Fig. 8. Rack Assembly for Longitudinal Loading

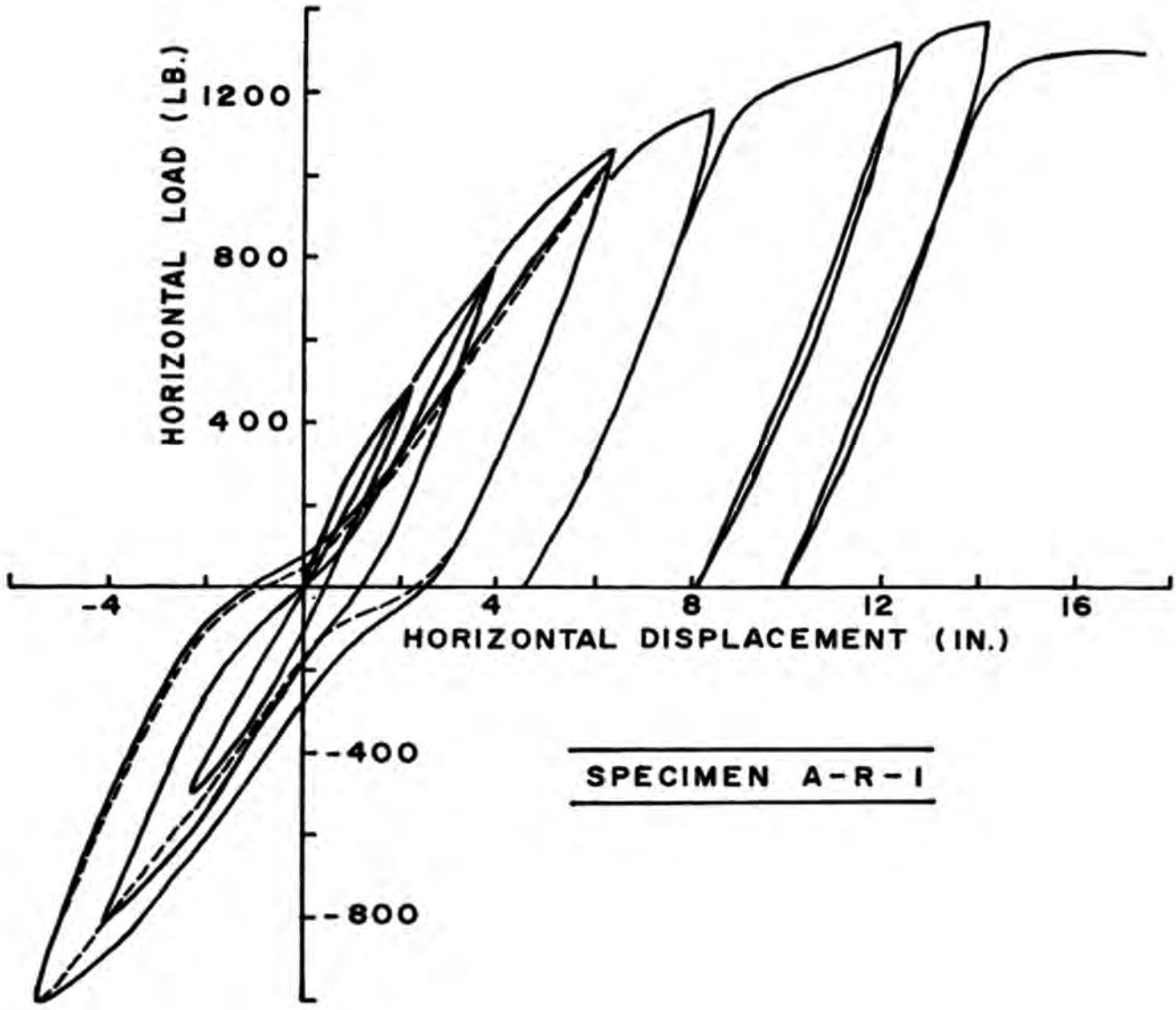

Fig. 9. H-δ Relationship for Rack Assembly -- Longitudinal Loading

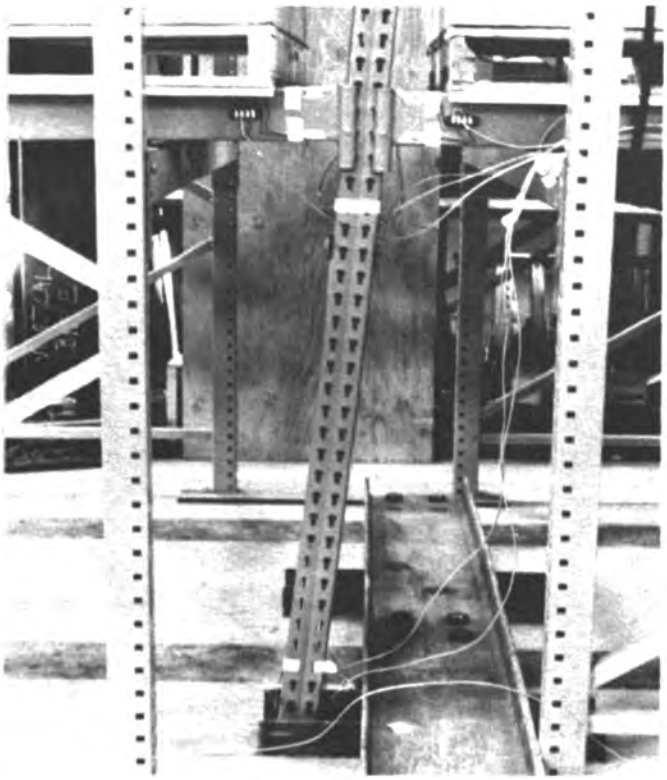

Fig. 10. Center Post of Specimen A-R-1 at Maximum Displacement

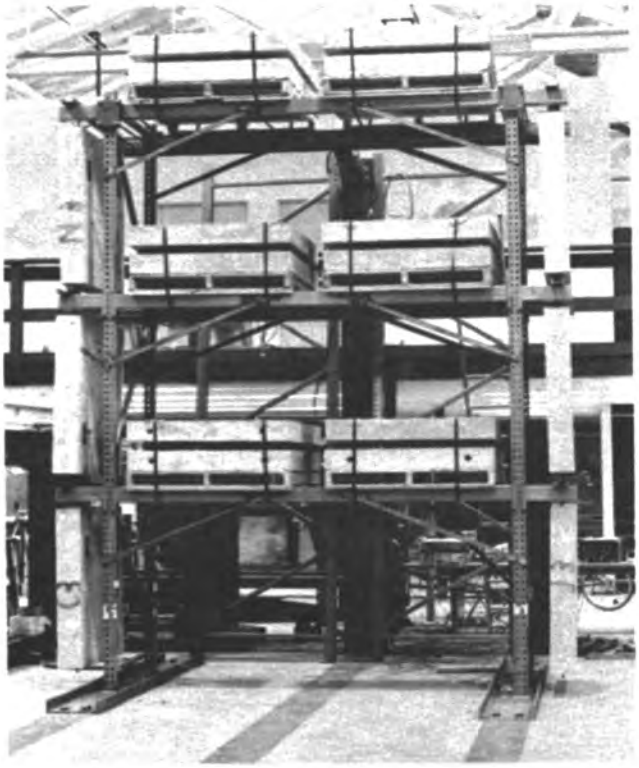

Fig. 11. Rack Assembly for Transverse Loading

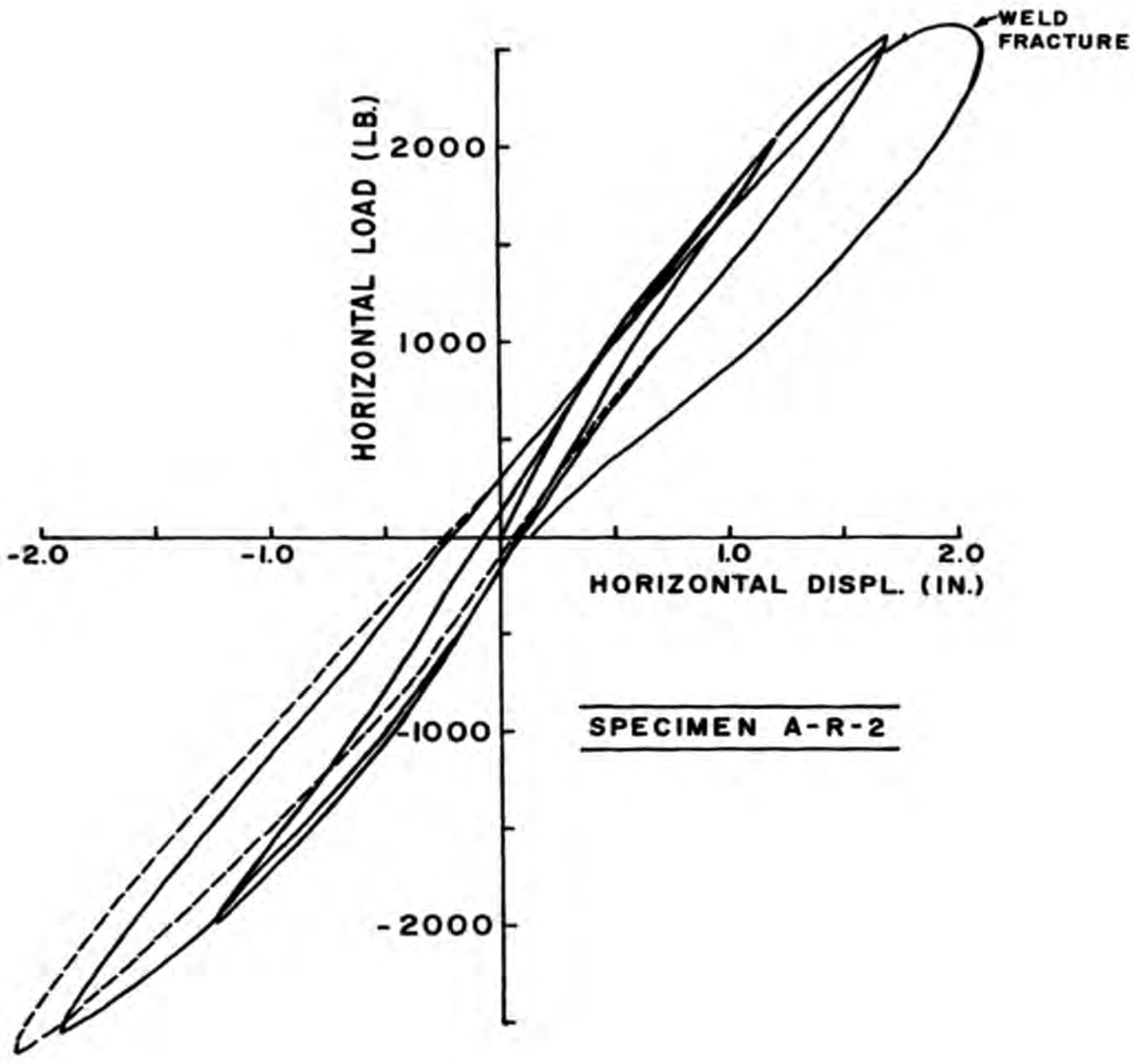

Fig. 12. H-δ Relationship for Rack Assembly -- Transverse Loading

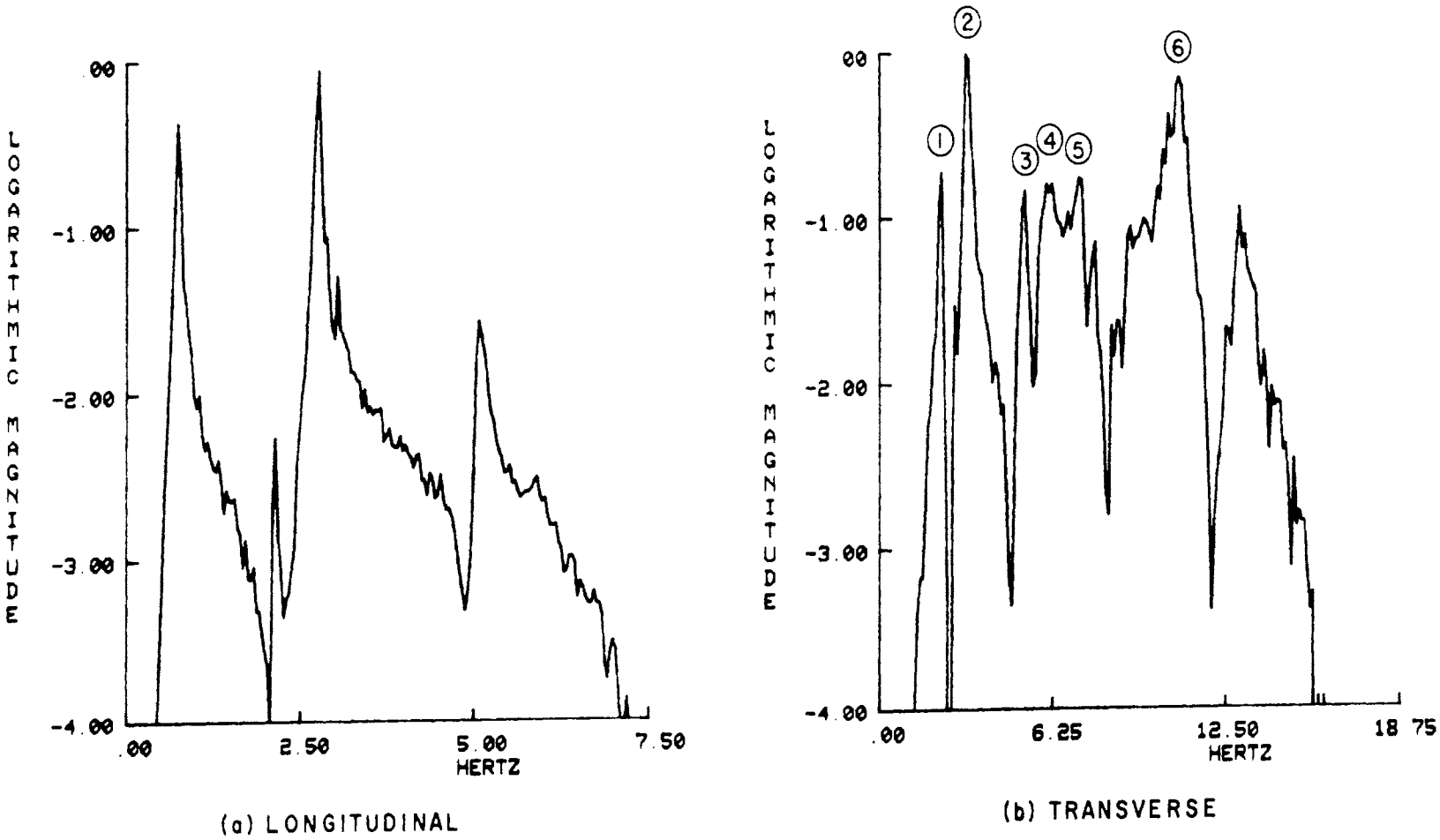

Fig. 13. Autopower Spectral Density Functions at Reference Point

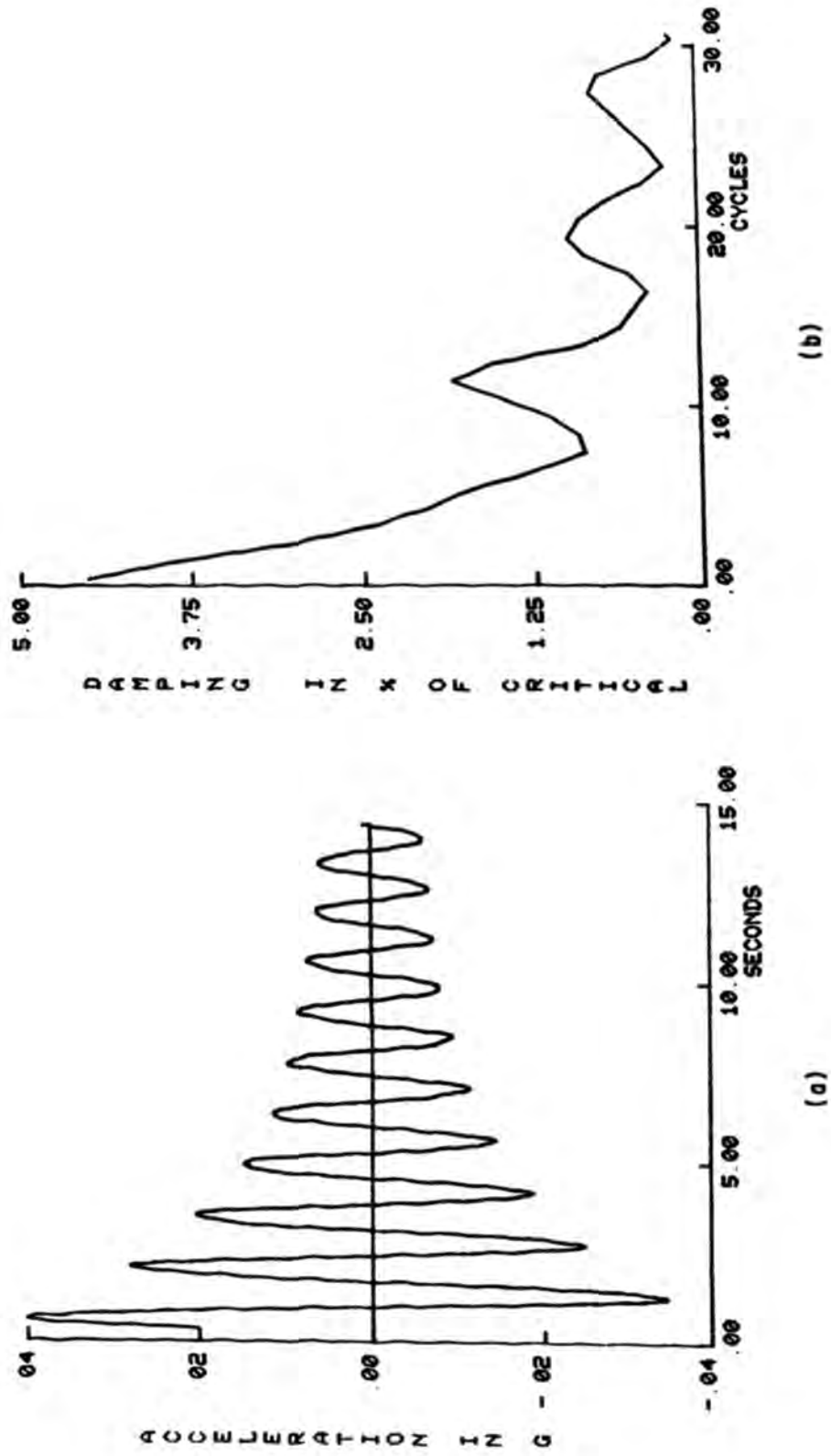

Fig. 14. Evaluation of Damping in First Longitudinal Mode